EXPERIMENTAL INVESTIGATION OF WATER AND MUD PUMPING DUE TO RAILROAD FOUNDATION LOADING

A Thesis

by

NICODEMO LUKE ACUNA

Submitted to the Graduate and Professional School of
Texas A&M University
in partial fulfillment of the requirements for the degree of

MASTER OF SCIENCE

Chair of Committee,	David H. Allen
Committee Members,	Robert Randall
	Roger Cordes
	Theofanis Strouboulis
Head of Department:	Sharath Girimaji

December 2022

Major Subject: Ocean Engineering

ABSTRACT

The purpose of this research is to investigate the mechanics of water and mud pumping in rail structures. From the conservation of mass model, it can be said that the volume of the railroad foundation will decrease under loading due to a decrease in void volume. A simple experiment was created to validate the mechanical assumption which determines the loading on the aggregate and associated settlement and water rise. The goal is to find a relation between the loading, settlement and water rise and develop a general one-dimensional model to predict the water level rise and compare it to experimental results. Additionally, the effects of cyclic loading on water and mud pumping were explored with and without fouling where fouling is defined as to be the result of voids filling with relatively finer material such as sand, soil, mud, or crushed ballast. The information gathered during this experiment will be used to help predict rail buckling in conjunction with research underway within the Texas A&M University Center for Railway Research.

CONTRIBUTERS AND FUNDING SOURCES

Contributors

This work was supported by a thesis committee consisting of Dr. Allen, Dr. Cordes, and Dr. Randall from the Department of Ocean Engineering and Dr Strouboulis from the Department of Aerospace Engineering. The model formulation depicted in this paper was done in part by David Allen of the Department of Ocean Engineering and Walter Haisler in the book Introduction to Aerospace Structural Analysis which was published in 1985.

All other work conducted for the thesis was completed by the student independently.

Funding Sources

Graduate study was supported by the means of a graduate research assistantship funded by Dr. Allen and the Texas A&M Transportation Institute.

TABLE OF CONTENTS

Page

LIST OF FIGURES

Page

INTRODUCTION

Railroads are of vital importance for the transportation of goods across the United States. 28 percent of U.S. Freight movement is by rail (U.S. Department of Transportation Federal Railroad Administration, 2022) with roughly 1.7 billion tons of goods moved each year (Association of American railroads, 2022). These goods come and go by port, thereby making the rail industry vital to the shipping industry. Track stability is therefore important to both industries as a derailment would disrupt the supply chain and perhaps even worse cause injuries and death.

When considering track stability, the buckling of the track is of importance for this research. Conditions that contribute to buckling include reduced track resistance, lateral alignment defects, and lowered rail neutral temperature (Kish, Mui, 2003). Contributions to reduced track resistance are the main concern in this thesis. The contributions studied will be predicting the water and mud rise which can cause permanent settlement, reduced friction between the ballast and crossties, and an unstable foundation, all of which can contribute to railroad buckling.

Past experiments have been previously undertaken to observe the stiffness and permanent deformation of ballast foundation as a function of load. Tamrakar and Nazarian (2020) studied both fouling the ballast and adding moisture, but they only observed the deformation and permanent settlement as shown in Figure 1 (Tamrakar & Nazarian 2020). Another study related to monotonic loading focused mainly on the force vs settlement but did not include the effect of water and water pumping (Key 1998).

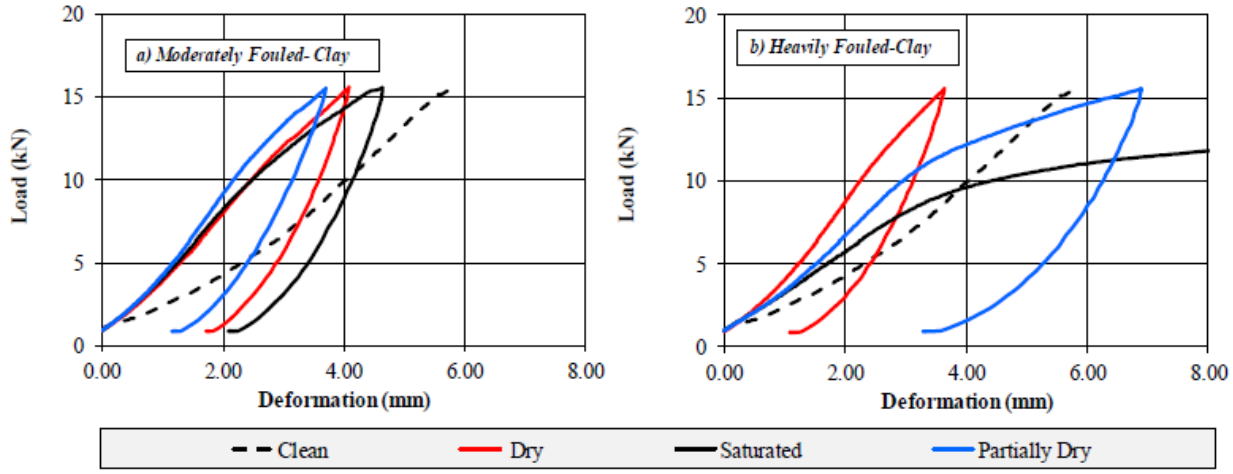

Figure 1: Load-Deformation Responses of Clay- Fouled Ballast (Tamrakar & Nazarian 2020)

Reprinted from Geosynthetica

Settlement of the track base vs cyclic loading has been explored as well. Many authors have conducted this type of experiment such as Pham and Dias who modeled the foundation settlement as a function of cycles (Pham and Dias, 2019). Their results are shown in Figure 2 which gives an idea of what to expect during the current experiment. However, whereas the information they gathered is informative they did not consider the water rise due to cyclic loading.

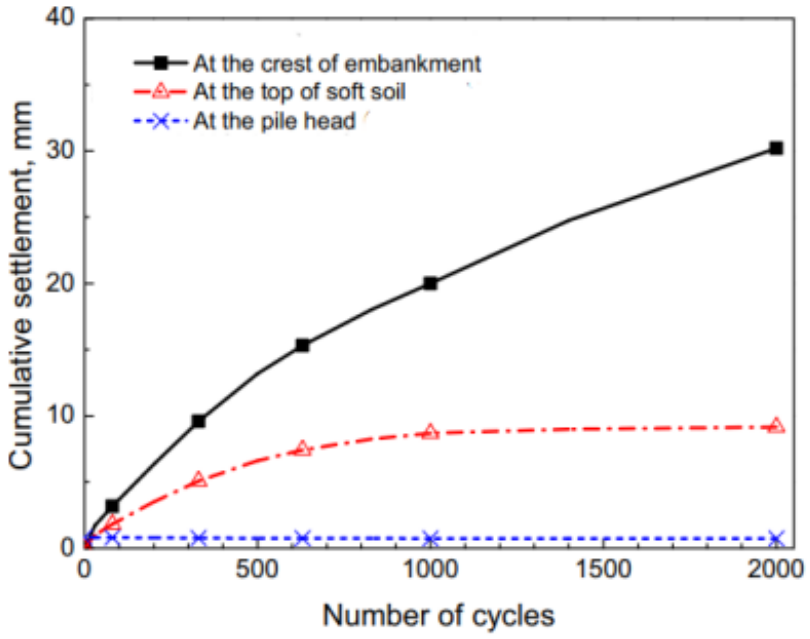

Figure 2: Settlement vs Number of Cycles (Pham and Dias, 2019) Reprinted from ascelibrary

When considering mud pumping and cyclic loading, Nguyen et al (2019) were successful in replicating the phenomenon as shown in Figure 3. They found that the amount of fines, excess water, and cyclic loads are the most significant factors affecting mud pumping. Additionally, they found that increasing excess pore pressure can accelerate the pumping affect. However, they did not assess the effects of fouling on mud pumping.

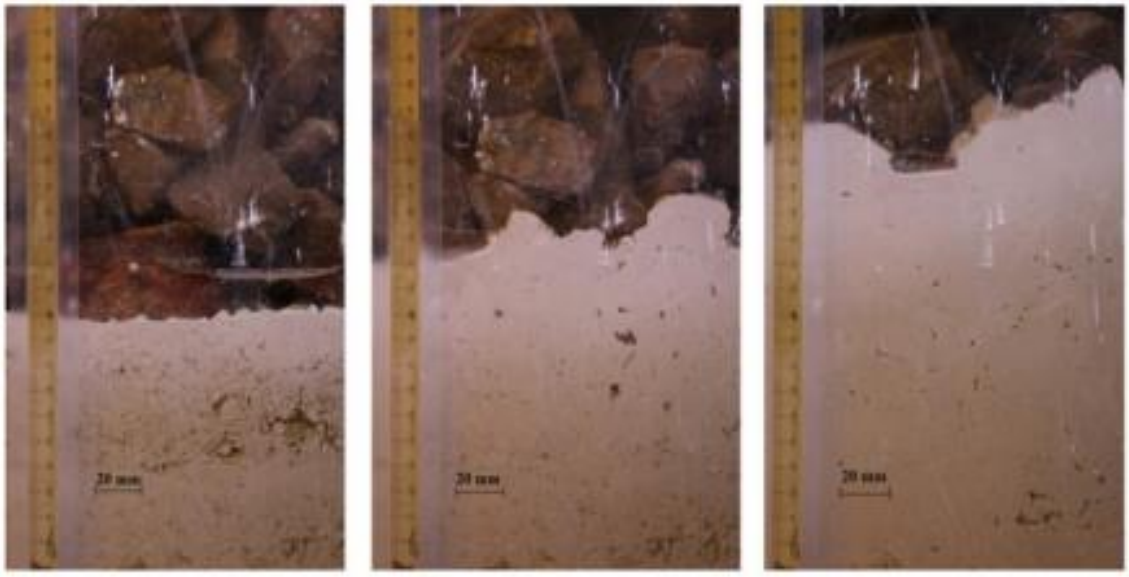

Figure 3: Upward Migration of Fines Due to Monotonic and Cyclic Loads (Nguyen, et al. 2019)

Reprinted from Australian Geomechanics Journal

As stated above, water and mud pumping occur when there is inadequate drainage, plentiful fines, and excess rain. In combination with both monotonic and cyclic loading the foundation may undergo settlement, thereby causing both water and mud to rise to the surface. This can in turn cause a decrease in friction between the crossties and ballast.

For the purpose of developing a model capable of predicting the effects of water pumping on track performance an experimental procedure is developed herein and compared to a simplified model based on the conservation of mass. Furthermore, whereas each of the previously performed experiments mentioned above is related to the overall issue of reduced track resistance, they either fail to address a saturated foundation with water and mud pumping or they don't include the effects of fouling due to cyclic loading. This thesis addresses these issues as they relate to track performance.

In summary, the experimental research observes the settlement of the foundation in relation to the applied loads both monotonically and cyclically. Additionally, the relation between the loading and rise in water and mud level will be explored. The information gathered from these experimental results will both help to validate the simplified water pumping model described herein and give insight into the physical behavior of water and mud pumping with and without fouling. The research provides better insight for understanding under what conditions water and mud pumping occur in track structure. Ultimately, the information gathered in this research contributes to an improved understanding of moisture related factors that contribute to rail buckling.

RESEARCH FRAMEWORK

Problem Statement

As previously stated, the purpose of this research is to develop a general one-dimensional water pumping model and validate it with experimental results. The experimental results are obtained by observing the water level rise of the saturated foundation as a function of the applied loading history. Additionally, the behavior and mechanics of water and mud pumping with and without fouling is observed and data is collected comparing the number of loading cycles versus the water and mud height. The data collected in this experiment is used to determine the relation between water level rise and monotonic loading, and to understand the behavior of the water and saturated soil under cyclic loading. From these results the general model for water pumping can be validated and the behavior of water and mud pumping can be better understood.

Methodology

The experiment is conducted in the Haynes Engineering Building (HEB) in room 006. In order to perform the experiments, a bin made of wood and plexiglass was constructed and filled with limestone ballast, water. For the cyclic loading test, soil was used. The purpose of the bin and material being to replicate a section of a railroad foundation normal to the direction of travel. A known force was then applied to the top surface of the foundation under both monotonic and cyclic loading conditions. Three types of tests are being conducted, including:

1) Monotonic loadings with increasing weight for a saturated foundation, and
2) 100-cycle test for a saturated foundation without fouling.
3) 100-cycle test for a saturated foundation with fouling.

Each test is performed 3 times for a total of 9 tests in order to assess the repeatability of the experimental procedure

The vertical modulus of the aggregate for the monotonic test can be determined by applying increasing monotonic loads and measuring the settlement from each load. The vertical modulus is defined as a measure of elasticity, equal to the ratio of the stress acting on the medium to the strain produced. The associated water level rise can also be observed for each load. The water and mud height change can be determined similarly by applying a cyclic load and measuring the change in height in 20 cycle increments during the 100-cycle test.

Both the monotonic and cyclic loading test are similar in terms of the underlying processes as described above. Applying a force to the top of the foundation causes it to settle. In doing so, the water level and the mud line rise due to a decrease in the void volume fraction. The above mechanics are described pictorially in Figures 4 and 5 below. Figure 4 shows the initial state of the foundation with an equally distributed force on a platten and no settlement. Figure 5 shows the resulting decrease in the void volume fraction, with an associated water level rise due to the applied loading.

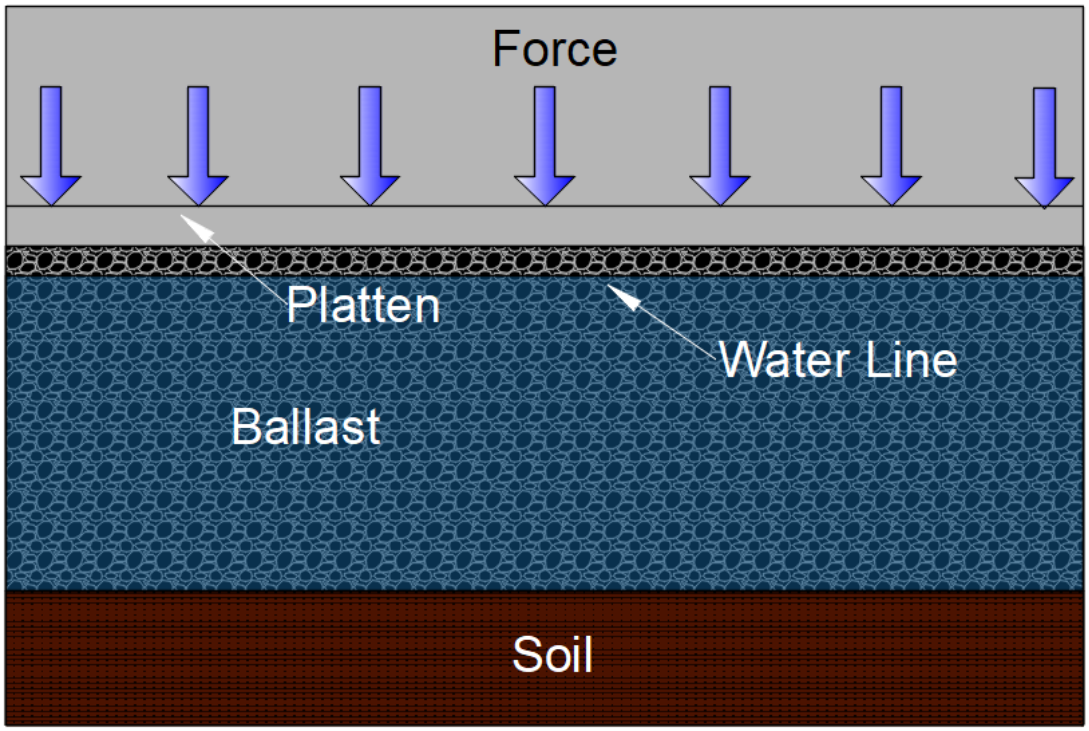

Figure 4: Water and Mud pumping Mechanics Initial State

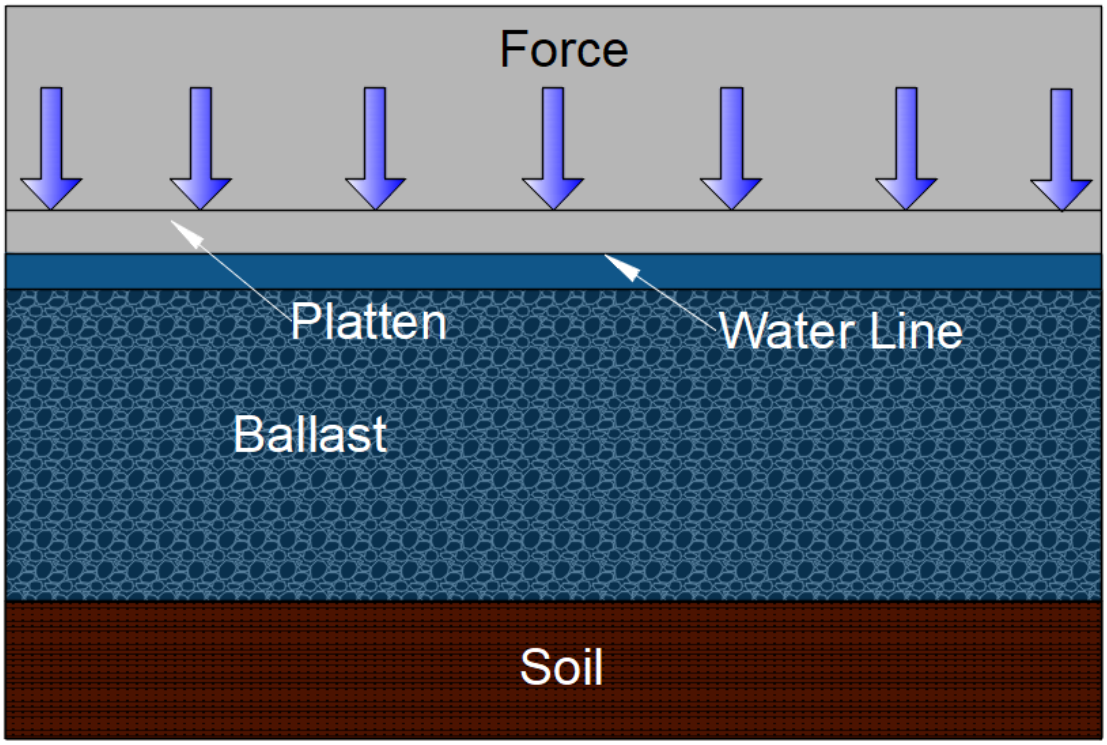

Figure 5: Water and Mud Pumping Mechanics

MODEL FORMULATION

Consider a box with dimensions of W (width), H (height), and D (depth) as shown in Figures 6 and 7 below. Within this box the only deformation allowed within the chamber is in the y (vertical) direction due rigid vertical walls within the compartment. Additional assumptions include the following: the material in the box is a porous Hookean material which in this case is the limestone ballast, the elastic modulus of air in the voids is negligible; and water is incompressible. It should also be said that for the purpose of modeling the material behavior of the aggregate, it is treated as a simply connected (spatially homogenous) continuum. Furthermore, body forces are neglected. The intention of this model is to determine the displacement fields in terms of the effective Young's modulus (E), and the effective Poisson ratio (ν) of the aggregate, as well as the pressure (P_0) applied by the horizontal platen. In order to determine the vertical component of the displacement field (v), the stress and strain components are predicted as well. The resulting model contains 15 unknowns comprised of 3 equilibrium equations, 6 strain displacement equations, and 6 stress-strain equations, as shown in Equation 1 below.

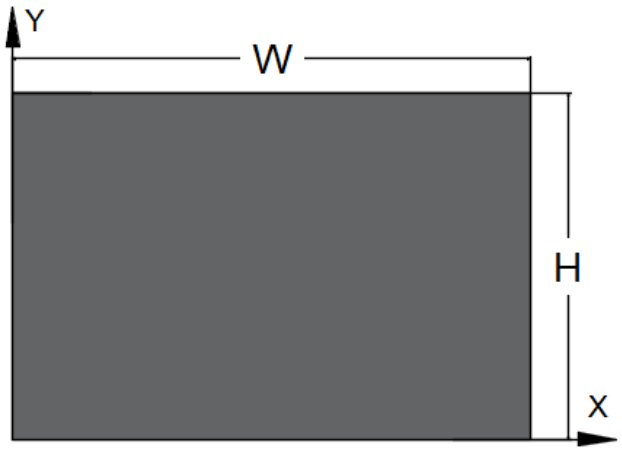

Figure 6: X-Y Plane View of Box Model

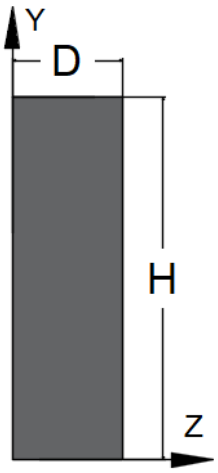

Figure 7: Y-Z Plane View of Box Model

$$Unknowns = u, v, w, \varepsilon_{xx}, \varepsilon_{yy}, \varepsilon_{zz}, \varepsilon_{xy}, \varepsilon_{xz}, \varepsilon_{yz}, \sigma_{xx}, \sigma_{yy}, \sigma_{zz}, \sigma_{xy}, \sigma_{xz}, \sigma_{yz} \quad (1)$$

With boundary conditions allowing the material to move freely in the y direction, it can be said that at all points in the body:

$$u = 0, \qquad \frac{\partial u}{\partial x} = \frac{\partial u}{\partial y} = \frac{\partial u}{\partial z} = 0 \quad (2)$$

$$v = unknown, \qquad \frac{\partial v}{\partial x} = \frac{\partial v}{\partial z} = 0 \tag{3}$$

$$w = 0, \qquad \frac{\partial w}{\partial x} = \frac{\partial w}{\partial y} = \frac{\partial w}{\partial z} = 0 \tag{4}$$

Equation 3 assumes that the interface between the ballast and vertical walls is frictionless, and therefore, the vertical displacement is constant in the horizontal plane. Substituting Equations 2 through 4 into the strain displacement relation gives Equations 5-8 below.

$$\varepsilon_{xx} = \frac{\partial u}{\partial x} = 0 \tag{5}$$

$$\varepsilon_{yy} = \frac{\partial v}{\partial y} \tag{6}$$

$$\varepsilon_{zz} = \frac{\partial w}{\partial z} = 0 \tag{7}$$

$$\varepsilon_{xy}, \varepsilon_{zy}, \varepsilon_{yz} = 0 \tag{8}$$

Equations 5-8 can be substituted into the 3-D Hookean strain formulation in Equation 9. This results in Equation 10 through 12. Because the only deformation is in the y direction, the 3-D Hookean strain formation below is simplified to just the 3 principal stresses as shown.

$$\begin{bmatrix} \sigma_{xx} \\ \sigma_{yy} \\ \sigma_{zz} \end{bmatrix} = \frac{E}{(1+\nu)(1-2\nu)} \begin{bmatrix} 1-\nu & \nu & \nu \\ \nu & 1-\nu & \nu \\ \nu & \nu & 1-\nu \end{bmatrix} \begin{bmatrix} 0 \\ \varepsilon_{yy} \\ 0 \end{bmatrix} \tag{9}$$

$$\sigma_{xx} = \frac{E\nu\varepsilon_{yy}}{(1+\nu)(1-2\nu)} \tag{10}$$

$$\sigma_{yy} = \frac{E(1-\nu)\varepsilon_{yy}}{(1+\nu)(1-2\nu)} \tag{11}$$

$$\sigma_{zz} = \frac{E\nu\varepsilon_{yy}}{(1+\nu)(1-2\nu)} \tag{12}$$

Equations 10-12 above are substituted into the equilibrium equations leading to Equations 13-15 below.

$$\frac{\partial \sigma_{xx}}{\partial x} = 0 \tag{13}$$

$$\frac{\partial \sigma_{yy}}{\partial y} = 0 \tag{14}$$

$$\frac{\partial \sigma_{zz}}{\partial z} = 0 \tag{15}$$

The evenly distributed pressure which acts on the y normal face can be introduced as shown in Equation 20 and then rearranged into Equation 21 below.

$$\sigma_{yy} = \frac{E(1-\nu)\varepsilon_{yy}}{(1+\nu)(1-2\nu)} = -P_0 \tag{20}$$

$$\varepsilon_{yy} = \frac{-P_0(1+\nu)(1-2\nu)}{(1-\nu)\mathrm{E}} \tag{21}$$

Given the relationship in Equation 22, Equation 21 can be integrated as shown as shown in Equation 23. Doing so leads to the Equation 24 below.

$$\frac{\partial v}{\partial y} = \varepsilon_{yy} = \frac{-P_0(1+\nu)(1-2\nu)}{(1-\nu)\mathrm{E}} \tag{22}$$

$$v = \int \frac{\partial v}{\partial y} dy = \int \varepsilon_{yy}\, dy = \int \frac{-P_0(1+\nu)(1-2\nu)}{(1-\nu)\mathrm{E}} dy \tag{23}$$

$$v = \frac{-P_0(1+\nu)(1-2\nu)}{(1-\nu)\mathrm{E}} y \tag{24}$$

Equation 24 above is the displacement (v) of the foundation surface in the y direction as a function of the pressure (P_0) and location (y) of the material. This model assumed that the material was homogenous but, that is not the case. This experiment and railroad foundation in general is composed of ballast which has voids. Because of these voids it can be said that the modulus of the control volume is a function of the void ratio of the rock volume (V_r) to the volume of the box (V_B). Introducing the variable $\bar{E}$ solved by Equation 24 below shows the relation. $\bar{E}$ can now be substituted back into Equation 24 which gives Equation 26 below. This now makes the displacement a function of the pressure (P_0), location (y), and dimensions (H, W, and D).

$$\bar{E} = \left(\frac{V_r}{V_B}\right) * E \tag{25}$$

$$v = \frac{-Po(1+\nu)(1-2\nu)}{(1-\nu)\bar{E}} y \tag{26}$$

Equation 26 can also be simplified to Equation 27. The material properties that are in equation 26 can appear implicitly within the value of the vertical stiffness (K).

$$v = \frac{-Po}{K} y \tag{27}$$

The change in void volume (ΔV_f) can now be calculated as a function of the original void volume fraction (V_f), the change in vertical height (v) and W and D shown in Equation 28, where the void volume fraction (V_f), given in Equation 29, is determined based on the known void ratio of the rock volume (V_r) to the box volume (V_B). This change in void volume (ΔV_f) can also be expressed as the volume of water that is pumped up (ΔV_w) as shown in Equation 30. Therefore, it can be said that the water height increase (ΔH_w) is equivalent to the vertical displacement of the aggregate but in the opposite direction as shown in Equation 31.

$$\Delta V_f = \left| V_f * v * W * D \right| \tag{28}$$

$$V_f = 1 - \frac{V_r}{V_B} \tag{29}$$

$$\Delta V_w = \left| V_f * v * W * D \right| \tag{30}$$

$$\Delta H_w = \frac{\Delta V_w}{W * D * V_f} = -v \tag{31}$$

EXPERIMENTAL SET-UP

The setup of the experiment is a box with emphasis on the 2-dimensional front face as shown in Figure 7. This box is elevated inside a water trough in case of any leakage and to allow for observations closer to eye level. Another smaller box with steel incased in it is used in conjunction with a jack to apply the load onto the foundation. Multiple cameras are used with the tripod to record the water and mud level for the experiments.

Foundation box

The foundation box is composed of pressure treated wood with a plexiglass face of 1.91 centimeters (0.75 inches) thickness. The internal dimensions of the box are 15.2 x 91.4 x 60.9 centimeters (6 x 36 x 24 inches). Three layers of flex seal was used on the interior of the box which included the bottom and side plywood panels. The flex seal is used to assist the waterproofing of the pressure treated wood and it gives abrasion resistance from the ballast. The box itself is contained inside a trough in case of any leaks. This trough is elevated as well to bring the view of the foundation closer to eye level.

Figure 8: Flex Seal Application on Interior Side and Bottom Panels

A front view of the foundation box is shown in Figure 9 and 10 below. The overall dimensions are shown for the interior and exterior of the box. In the AutoCAD drawing, the red pieces represent the lateral supports which helps to prevent the plexiglass from deflecting. The black section represents the interior part of the box that has been flex sealed. The hex hatched section in the drawing represents the interior vertical beam which helps hold the plexiglass in place along with an industrial adhesive, E6000.

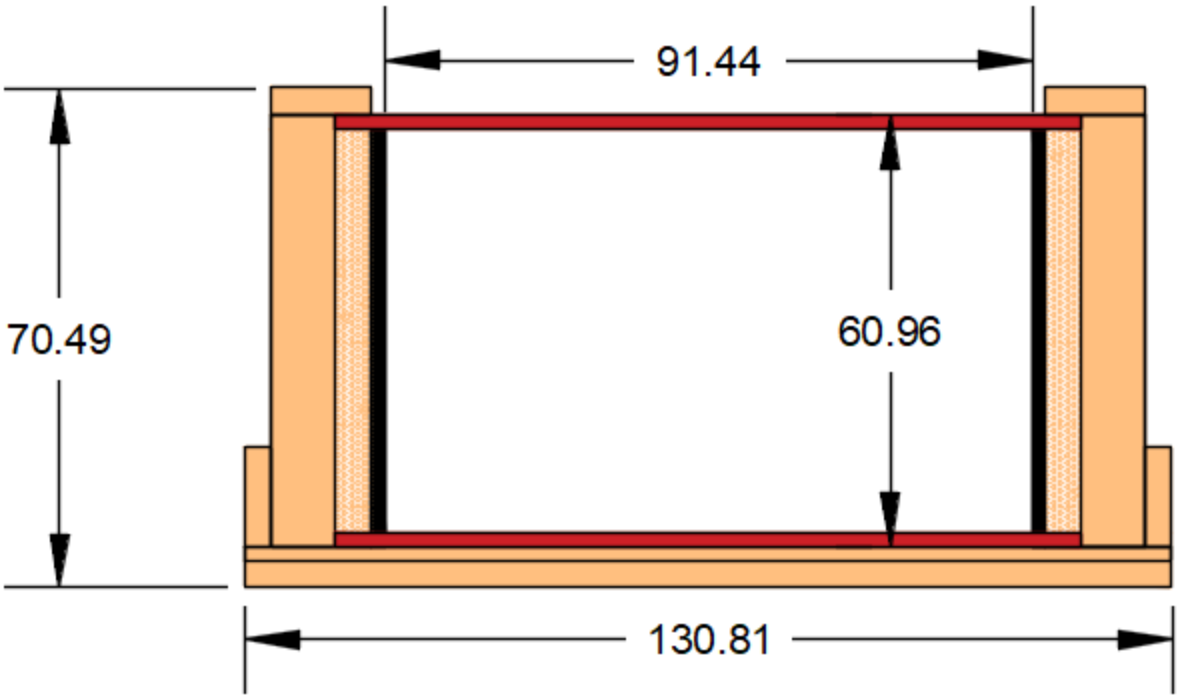

Figure 9: AutoCAD Drawing of the Foundation Box Showing Exterior and Interior Dimensions (Centimeters)

Figure 10: Picture of Foundation Box

A side view of the foundation box is shown in Figure 11 below with the external dimensions. The plexiglass is highlighted in teal/baby blue and is sandwiched between two vertical beams. E6000 is used in between the plexiglass and the beams to assist with waterproofing. These vertical beams are held in place by two support pieces at the top of the box and the bottom. These supports help to minimize deflections. Figure 12 below shows the entire experimental setup which includes the elevated trough, foundation box, load container, and camera setup.

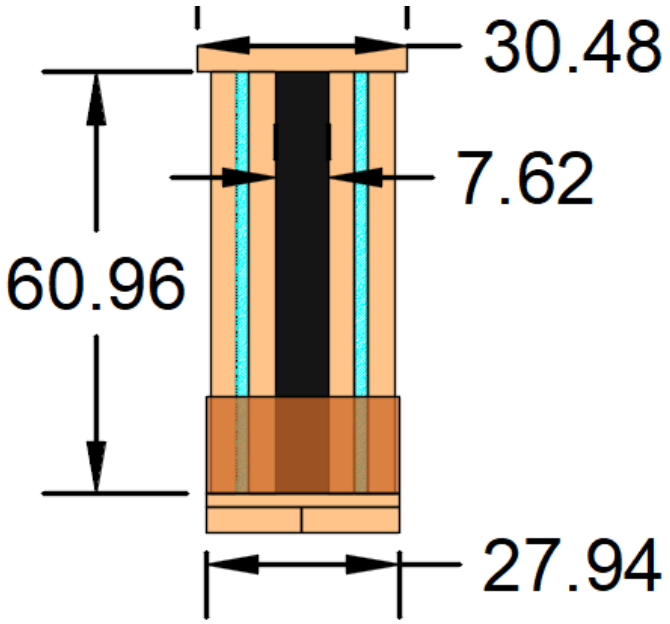

Figure 11: AutoCAD Drawing of the Foundation Box Side - Exterior Dimensions (Centimeters)

Figure 12: Picture Showing the Full Experimental Setup of the Foundation Box with the Load

Foundation Material

The foundation material consists of 2.54-centimeter (1 inch) limestone ballast and water. Approximately 90.72 Kilograms (200 pounds) of ballast was used to fill the bin for these experiments with slight variation between each of the tests. This is due to the ballast being replaced after each test. Water is the last component of the foundation which again varies slightly. Overall, the water level is a few centimeters below the foundation surface prior to loading.

Load and jack

The load being applied is composed of steel triangles as shown in Figure 13 which vary in weight of 20.5-25 Kilograms. The steel triangles used were weighed three times, and the average weight was taken. The weights are contained in a wooden box as well with exterior dimensions of 13.97 x 90.17 x 38.1 centimeters (5.5 x 35.5 x 15 inches) as shown in Figure 14. These exterior dimensions allow for the load to be sufficiently spread out across nearly the entire surface of the foundation. There are two holes on each side of the box where a chain goes through that allows the box to be connected to the jack. The jack itself is a mobile engine hoist with a two short ton capacity that can be wheeled underneath the trough. The entire loading apparatus is shown in Figure 15.

Figure 13: Picture of the Steel Weight Being Used for the Load

Figure 14: Picture Showing Container Used to Contain the Load

Figure 15: Picture Showing the Jack and Container box

Camera setup

A tripod is setup to record the experiments at both the water and mud level. The height of each camera is level to the mud and water line. For the camera to fit between the box and jack, the 2 front legs of the tripod must be placed onto the part of the structure that holds the trough in place. Because of this there is some vibration during the loading that causes vibration in the video recordings. To reduce the vibration from the loading within the camera recording, a rubber mat was placed underneath each of the two legs as a damper.

EXPERIMENTAL PROCEDURE

The experiment was conducted in three separate parts as stated before. The first part is the monotonically loaded foundation, and the other two parts are the cyclic loading for fouled and non-fouled ballast. The experiment is meant to collect data for the foundation stiffness, water level rise, and mud height rise.

Monotonic loading

For the first test, the foundation needs to be added and given an initial settlement. The foundation is then saturated to where the water level is a few centimeters below the surface. The foundation is then initially settled by hand and with the empty box that holds the steel. The test itself begins with the empty load box lowered onto the foundation. Next, two steel triangles are added onto either side of the box and the settlement and associated water level rise is recorded. An additional two triangles are added and again the settlement and associated water level rise is recorded. The loading procedure was repeated for eight steel triangles. These actions were repeated two more times for a total of three test. Before starting a new test, the ballast is taken out and new material is placed inside.

Cyclic loading

The test of the non-fouled ballast is similar to the monotonic loading test. Fresh ballast is placed inside the box and the foundation is initially settled. This is done again by hand and with the box that holds the steel. The foundation is then saturated to where the water level is roughly a few centimeters below the surface. Two cameras are setup to capture the water and mud line throughout the test. These cameras are setup level to both the areas to get an accurate visual representation. The load is applied at a frequency of 0.1 Hz for 100 cycles. Each cycle is

represented by the load being raised 2.5-5 centimeters above the surface and then released by the jack. From the recordings the settlement and water and mud height can be determined at the various cycles. Again, the ballast is replaced and initially settled before the remaining test are conducted.

Fouling

The fouling of the ballast consisted of creating a slurry mixture and mixing it with the first bottom layers of aggregate. The slurry is composed of a clayey-loamy soil with a 2:1 water to soil ratio. The slurry is added in layers by first laying a small fresh layer of ballast followed by the slurry. This is repeated until there is no remaining slurry.

Data Acquisition

For each test, the settlement and change in both water and mud height are determined with the use of the video cameras. The first monotonic test video captured the change in height of the foundation at each different load. For the cyclic loading, screenshots at the 0, 20, 40, 60, 80, and 100 cycle mark. Similarly, the video for the monotonic loads, screenshots were taken at each different load. Each screenshot can be uploaded into an image processing program called ImageJ. From here the water and mud height were calculated by first scaling the pixels based off the known distances captured in the images. An area was then determined by tracing the top of the water or mud line, the edges of the image, and across a specified height. Knowing the width of the highlighted area, an average height was then calculated for each image. The height change was then recorded for each cycle or load.

RESULTS AND DISCUSSION

Monotonic Loading

The monotonic loading test was successful in acquiring data for the settlement and water level rise with an increasing applied load. While there was some variation between the three test, each one behaved similarly. Figure 16 below shows the three monotonic loading tests in comparison to the water pumping model. As can be seen there is some difference between the model and experimental results, but they are similar. The percent error between the model and experimental results is roughly 10%.

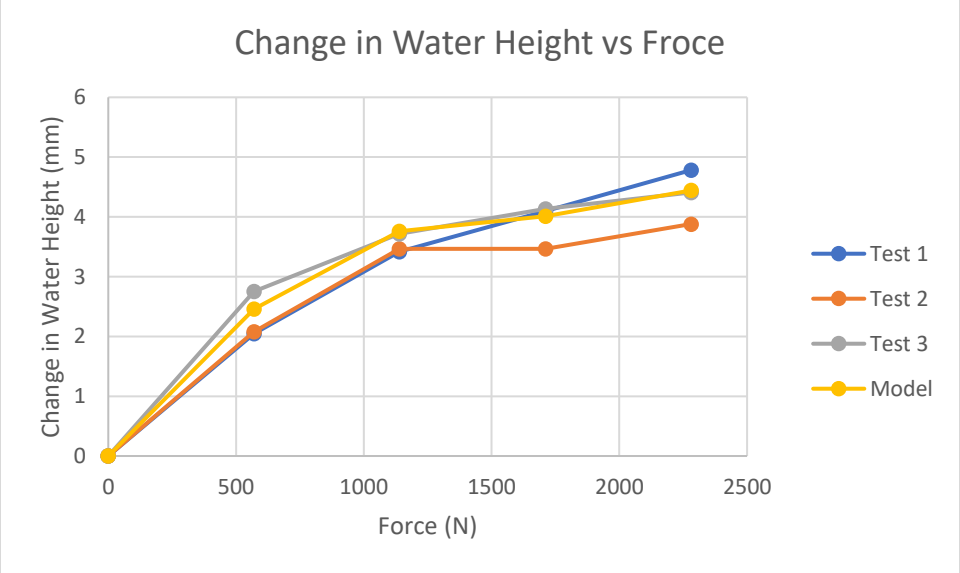

Figure 16: Monotonic Loading- Force vs Change in Water Height

The cause of the error can be contributed to a few things. First the model made assumptions that there were no deflections in the X or Z coordinates. In reality, the plexiglass face which is normal to the Z axis does have some deflection as the foundation is loaded. The magnitude of which is unknown, but it does contribute to the error. Additionally, the ballast is coarse and rough which inherently causes friction between the material. This interaction prevents

the foundation from deforming at a constant rate with respect to the applied force while the model assumes that the ballast will deform constantly.

Cyclic Loading – Water Pumping

The non-fouled and fouled graphs are shown in Figures 17 and 18 below. From Figure 17 below one can see that the trend in each test is similar but there is a large variation between the different tests. This will be discussed later below. There is not as much variation between the tests in Figure 18 in comparison to the non-fouled test shown in Figure 17.

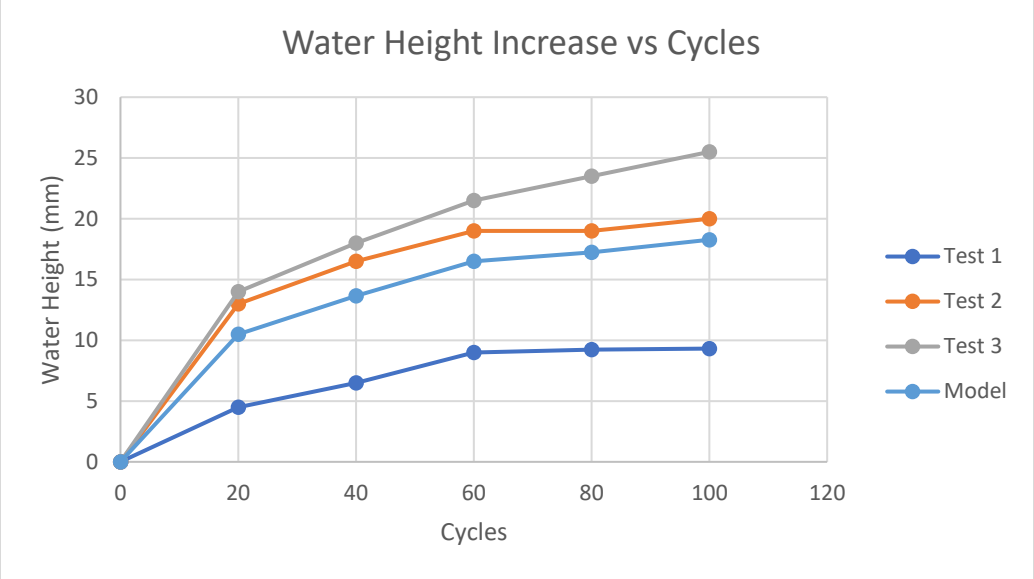

Figure 17: Cyclic Loading – Non-Fouled Water Height Increase

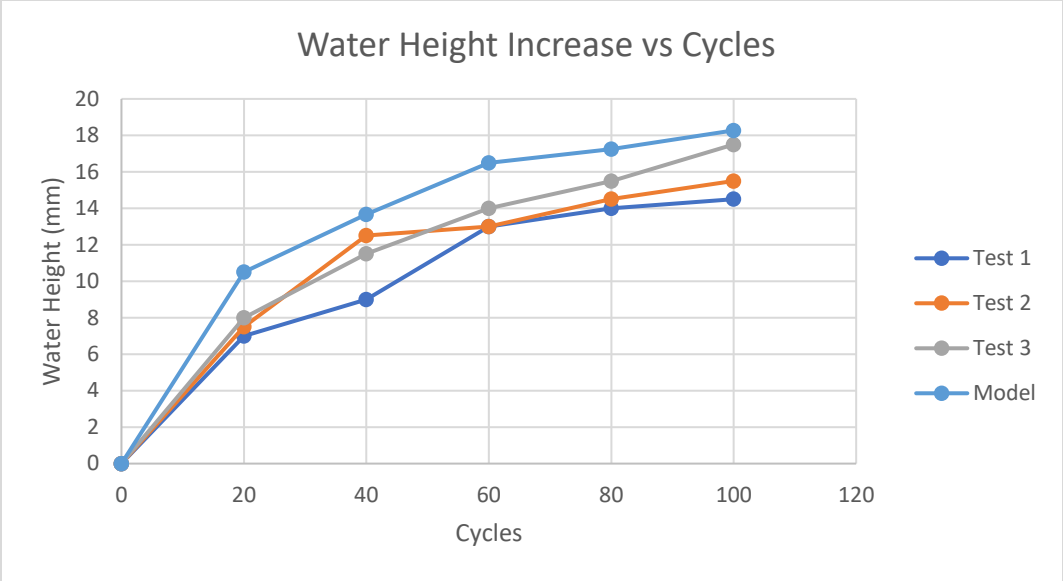

Figure 18: Cyclic Loading – Fouled Water Height Increase

Most of the water pumping test in relation to cyclic loading behaved similarly. The major outlier was test 1 in the non-fouled category shown in Figure 17. The water level did not rise much in comparison to the other test. Now the question as to why that is can be answered with the introduction of randomness. As mentioned before after each test the ballast was removed and replaced with fresh material. When the new material is added the ballast is oriented at random and even though an initial settlement is given there are possibilities of having various amounts of porosity which thereby affect the modulus.

Figure 19 below shows the water level rise for the fouled and non-fouled test as well as the model comparison. Observing the figure one can see that the fouled and non-fouled test behaved similarly but the fouled test showed less of a water height increase. This can be explained by the fact that mud is compressible, so the slurry mixture in the fouled ballast causes a decrease in water height increase. The model does show some similarities to both test in terms of the pattern. Yet the predictive model does contain some error in the values which is roughly 22% in comparison to the non-fouled case. This error is even greater when comparing to the

fouled test. This additional error when comparing to the fouled case can be attributed to the fact that the model itself does not account for fouling.

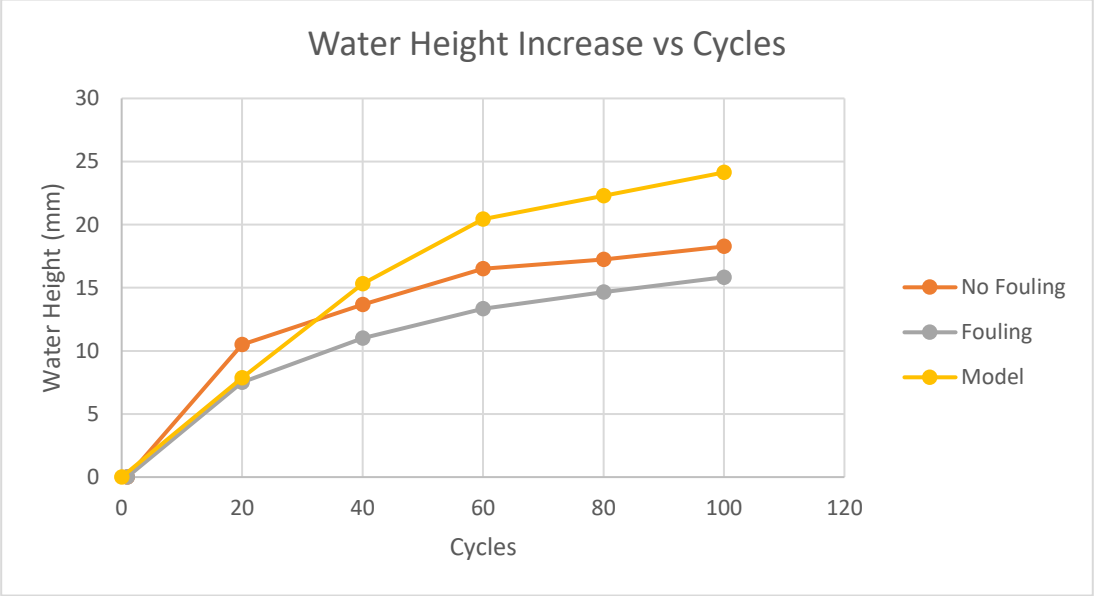

Figure 19: Cyclic Loading – Water Height Increase Comparison

Cyclic Loading – Mud Pumping

Mud pumping was explored for this research as well and these results are shown in Figure 20 below with the fouled ballast. As one can see there was no distinguishable pattern whatsoever in this experiment. This can be partially attributed to the fact that the changes were so miniscule over the 100 cycles that it was near impossible to get an accurate data set. Because of this the mud pumping test were not successful for this experiment over the 100 cycles.

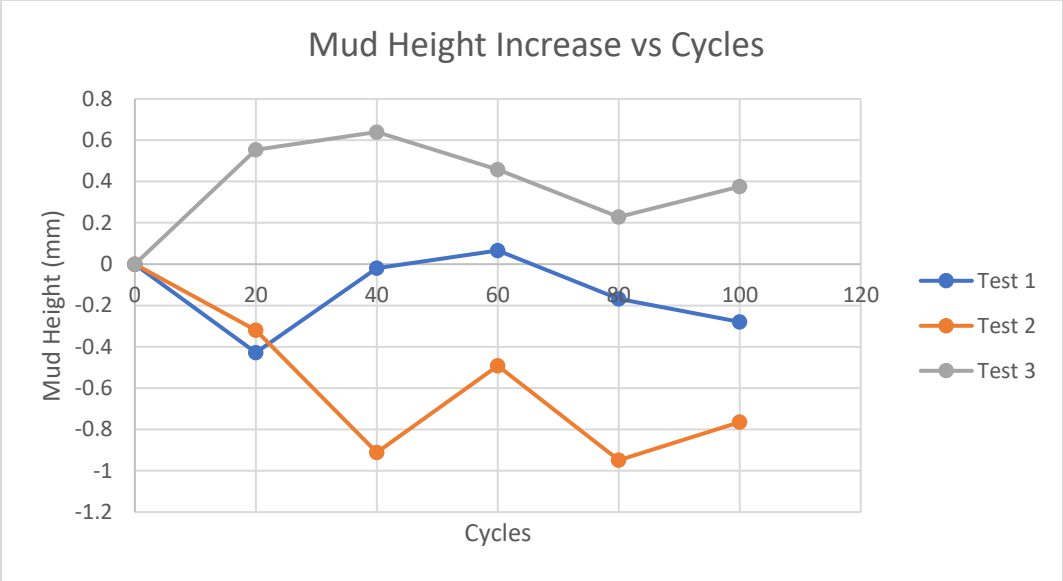

Figure 20: Cyclic Loading - Fouled Mud Height Increase

CONCLUSION

In this thesis, a mathematical model for water pumping was developed and compared to experimental results. Because there was only a 10% error between the model and experimental results there is now a basis for continuing this research and further developing this model. Additionally, it was found that the model can be applied to the cyclic loading case when there is no fouling. It was also found that fouling the ballast causes the amount of water being pumped to decrease. When observing the mud pumping, it was found that for a duration of only 100 cycles there was no significant change. In fact, it was almost impossible to obtain a reliable reading. Therefore, no accurate information about mud pumping as a function of cycles was determined.

IMPROVEMENTS AND FUTURE WORK

As a result of these experiments there are a few areas that could use improvements. The currently developed model only accounts for non-fouled ballast. In reality there are miles of track that contains fouled ballast which can contribute to water pumping so there is need to further develop this model to account for fouling. Furthermore, the data acquisition method needs to be more accurate. The water height measurements were taken visually and had an accuracy of ± 0.5 millimeters. This could be improved with the use of other devices to better measure the water height. To reproduce experimental results closer to the water pumping model the plexiglass could have been better supported to prevent lateral deflections. The experiment was limited in the load size and application. If a larger load was available from an MTS machine which could apply it at a constant rate, then the experimental results could provide a more accurate comparison to the model.

Because of the complexity of these mechanics there are several parameters that could be changed. In the scope of the current thesis, future work for this experiment could include changing the ballast to soil ratio of the foundation to see if there is any noticeable difference. Additionally different soil types could be used to see how the mud pumping changes based on the characteristics of the soil such as the liquid limit or plastic limit. Finally, performing a greater number of cycles at various loads would be useful in understanding the water and mud pumping characteristics.

REFERENCES

Allen, D. H., & Haisler, W. E. (1985). *Introduction to aerospace structural analysis*. J. Wiley and Sons.

Berggren, Eric. "Railway Track Stiffness Dynamic Measurements and Evaluation for Efficient Maintenance." *KTH Royal Institute of Technology*, 2009.

"Freight Rail in Your State." *Association of American Railroads*, www.aar.org/data-center/railroads-states. Accessed 4 Apr. 2022.

"Freight Rail Overview." *U.S. Department of Transportation Federal Railroad Administration*, railroads.dot.gov/rail-network-development/freight-rail-overview. Accessed 4 Apr. 2022.

Kelly, C., Tamrakar, P., & Nazarian, S. (2020, February 4). *Permanent deformation and stiffness of fouled ballast based on static and impact load tests*. Geosynthetica. Retrieved May 12, 2022, from https://www.geosynthetica.com/deformation-stiffness-fouled-ballast-tests/

Key, Andrew John. *Behaviour of two layer railway track ballast under cyclic and monotonic loading*. (1998). University of Sheffield. PhD thesis. *White Rose eTheses Online*, https://etheses.whiterose.ac.uk/14504/

Kish, Andrew, and Wesley Mui. "Track Buckling Research." *Repository and Open Science Access Portal*, 7 Sept. 2003, https://rosap.ntl.bts.gov/view/dot/11985. Accessed 5 Apr. 2022.

Nguyen, Thanh, Buddhima Indraratna, Richard Kelly, Nghi Minh Phan, and Ferry Haryono. "MUD PUMPING UNDER RAILTRACKS: MECHANISMS, ASSESSMENTS AND SOLUTIONS." *Australian Geomechanics Journal*, vol. 54, no. 4, 2019, pp. 59–80.

Pham, Hung V., and Daniel Dias. “3D Numerical Modeling of a Piled Embankment under Cyclic Loading.” *International Journal of Geomechanics*, vol. 19, no. 4, Apr. 2019, https://doi.org/10.1061/(asce)gm.1943-5622.0001354. Accessed 5 Apr. 2022.

Rasband, W.S., ImageJ, U. S. National Institutes of Health, Bethesda, Maryland, USA, https://imagej.nih.gov/ij/, 1997-2018